arXiv:1101.0701v1 [astro-ph.CO] 4 Jan 2011

Filter Design for the Detection/Estimation of the Modulus of a Vector. Application to Polarization Data

Francisco Argüeso[a], José Luis Sanz[b], Diego Herranz[b]

[a]*Departamento de Matemáticas, Universidad de Oviedo, 33007, Oviedo, Spain*
[b]*Instituto de Física de Cantabria (CSIC-UC), 39005, Santander, Spain*

Abstract

We consider a set of M images, whose pixel intensities at a common point can be treated as the components of a M-dimensional vector. We are interested in the estimation of the modulus of such a vector associated to a compact source. For instance, the detection/estimation of the polarized signal of compact sources immersed in a noisy background is relevant in some fields like Astrophysics. We develop two different techniques, one based on the Maximum Likelihood Estimator (MLE) applied to the modulus distribution, the modulus filter (ModF) and other based on prefiltering the components before fusion, the filtered fusion (FF), to deal with this problem. We present both methods in the general case of M images and apply them to the particular case of three images (linear plus circular polarization). Numerical simulations have been performed to test these filters considering polarized compact sources immersed in stationary noise. The FF performs better than the ModF in terms of errors in the estimated amplitude and position of the source, especially in the low signal-to-noise case. We also compare both methods with the direct application of a matched filter (MF) on the polarization data. This last technique is clearly outperformed by the new methods.

Keywords: Filters, image processing, matched filters, object detection, polarization, astronomy.

1. Introduction

The detection and estimation of the intensity of compact objects –i.e. signals with a compact support either in time or space domains– embedded in a background plus instru-

Email address: herranz@ifca.unican.es (Diego Herranz)

mental noise is a problem of interest in many different areas of science and engineering. A classic example is the detection of point-like extragalactic objects such as galaxies and galaxy clusters in sub-millimetric Astronomy. Regarding this particular field of interest, different techniques have proven useful in the literature. Some of the proposed techniques are frequentist, such as the standard matched filter [1], the matched multifilter [2] or the recently developed matched matrix filters [3]. Other frequentist techniques include continuous wavelets like the standard Mexican Hat [4] and other members of its family [5] and, more generally, filters based on the Neyman-Pearson approach using the distribution of maxima [6]. All these filters have been applied to real data of the Cosmic Microwave Background (CMB), like those obtained by the WMAP satellite [7] and CMB simulated data [8] for the experiment on board the *Planck* satellite [9], which has recently started operations. Besides, Bayesian methods have also been recently developed [10]. Although we have chosen the particular case of sub-millimetric Astronomy as a means to illustrate the problem of compact source detection, the methods listed above are totally general and can be used to any analogous image processing problem.

In most cases one is interested only in the intensity of the compact sources. In other cases, however, there are other properties of the signal that may be of interest. Such is the case, for example, of sources that emit electromagnetic radiation that is at least partially polarized. Polarization of light is conventionally described in terms of the Stokes parameters Q, U and V. Let us consider a monochromatic, plane electromagnetic wave propagating in the z-direction. The components of the wave's electric field vector at a given point in the space can be written as

$$\begin{aligned} E_x &= a_x(t)\cos\left[\omega_0 t - \theta_x(t)\right] \\ E_y &= a_y(t)\cos\Big[\omega_0 t - \theta_y(t)\Big]. \end{aligned} \tag{1}$$

If some correlation exists between the two components in the previous equation, then the wave is *polarized*. The Stokes parameters are defined as the time averages

$$\begin{aligned} I &\equiv \langle a_x^2\rangle + \langle a_y^2\rangle, \\ Q &\equiv \langle a_x^2\rangle - \langle a_y^2\rangle, \\ U &\equiv \langle 2a_x a_y \cos\Big(\theta_x - \theta_y\Big)\rangle, \\ V &\equiv \langle 2a_x a_y \sin\Big(\theta_x - \theta_y\Big)\rangle. \end{aligned} \tag{2}$$

The parameter I gives the intensity of the radiation which is always positive, while the other three parameters define the polarization state of the wave and can have either sign. Q and U are the linear polarization parameters and V indicates the circular polarization of the wave. Unpolarized radiation is described by $Q = U = V = 0$.

While the total intensity of the wave is independent of the orientation of the x and y axes, the values of the other Stokes parameters are not invariant with respect to changes of the orientation of the receivers. On the other hand, the *total polarization*, defined as

$$P \equiv \sqrt{Q^2 + U^2 + V^2}, \tag{3}$$

is invariant with respect to the relative orientation of the receivers and the direction of the incoming light, and therefore it is a quantity with a clear physical meaning. For the case of purely linear polarization, $V = 0$ and the previous expression reduces to $P \equiv (Q^2 + U^2)^{1/2}$. Note that in order to get P from its components Q, U, V it is necessary to perform a non-linear operation.

Although strictly speaking Q, U and V are the components of a tensor, the invariant combination (3) gives a quantity that can be seen as the modulus of a vector. In this paper we will introduce a methodology that can be applied to any problem in which a set of images contain signals whose individual intensities can be considered as the components of a vector, but where the quantity of interest is the modulus of such a vector. For illustrative purposes, throughout the paper we will use as an example the case of light polarization, but the methods we will introduce are not limited to the example. Another possible application could be the determination of the modulus of a complex-valued signal. For example, in [11] the case of the estimation of the modulus of a complex-valued quantity whose components follow a Gaussian distribution was addressed. The techniques presented in their paper are related to our methods, but restricted to the two-dimensional case. In [12], four methods: MLE estimator, median estimator, mean estimator and Wardle and Kronberg's estimator [13] are applied to the estimation of polarization (two-dimensional case). However, these methods are applied in the cited paper to a single data and cannot be, except for the MLE, generalized to the detection of a signal with a given profile in a pixelized image, as considered in our paper. This is due to the fact that these methods lead to a system of possibly incompatible equations.

Going back to the case of point-like extragalactic objects in sub-millimetric Astronomy, the polarization of the sources plays and important role in the cosmological tests derived from CMB observations. Standard cosmological models predict that CMB radiation is linearly polarized. However, some cosmological models predict in addition a possible circular polarization of CMB radiation [14]. In order to better constrain the cosmological model with observations, it is crucial to determine the degree of polarization of not only the CMB radiation but also the other astrophysical sources whose signals are mixed with it. For an excellent review on CMB polarization, see [15]. We have treated the application to the detection of linearly polarized sources in CMB maps elsewhere [16], but it is known that extragalactic radio sources can also indeed show circular polarization [17]. Besides, circular polarization occurs in many other astrophysical areas, from Solar Physics [18] to

interstellar medium [19], just to put a few examples. Therefore, in this paper we aim to address the general case of linear plus circular polarization of compact sources.

In the general case we have three images Q, U and V. Different approaches can be used to deal with detection/estimation of point-like sources embedded in a noisy background. On the one hand, one can try to get the source polarization amplitude A directly on the P-map. In this approach, we will consider one filter, obtained through the MLE applied to the modulus distribution (ModF). On the other hand, we can operate with three matched filters, each one on Q, U and V followed by a quadratic fusion and square root (FF). We are trying to compare the performance of the two techniques for estimating the position and polarization amplitude of a compact source. Of course, in the case we have only the map of the modulus of a vector and the components are unknown, the FF cannot be applied but we can still use the ModF. Finally, we also apply a matched filter (MF) directly on the P-map and compare this simple method with the two new methods introduced in this paper.

In Section 2 we will develop the methodology for the case of M images, because of the possible interesting applications to the general M-dimensional case and in particular to the 3-dimensional case (polarization). In Section 3 we will show the results when applying these techniques to numerical simulations of images of Q, U and V that are relevant for the detection of compact polarized sources in Astrophysics. Finally, in Section 4 we give the main conclusions.

2. Methodology

2.1. The case of M images

To develop our methodology, let us consider M images with intensities $d_j(\vec{x})$ at each point $\vec{x}$ of their common domain, $j = 1, \ldots, M$. Hidden in these images there is an unknown number of signals. In this work we consider signals with compact support ('compact sources' hereinafter), as for example galaxies in CMB polarization images. For simplicity, let us consider the case of a single compact source embedded in the images. We will assume a linear model

$$d_j(\vec{x}) = A_j \tau(\vec{x}) + n_j(\vec{x}). \tag{4}$$

In this equation, the source is characterized by amplitudes A_j in each image and by a spatial profile $\tau(\vec{x})$ that is the same for the M images. This last condition is satisfied when the instrument resolution is much higher than the source scale . The source is immersed in noise $n_j(\vec{x})$ that is Gaussian and independently distributed with zero mean and dispersion $\sigma(\vec{x})$. Then the distribution of $d_j(\vec{x})$ is Gaussian with mean $A_j\tau(\vec{x})$ and dispersion $\sigma(\vec{x})$. We will consider that the noise is non-stationary but the dispersion is the same for

the different images at the same pixel. These conditions are typical in polarization images. By construction, the total polarization map $P(\vec{x}) \equiv (\sum_j d_j^2(\vec{x}))^{1/2}$ includes a source characterized by a total polarization amplitude $A \equiv (\sum_j A_j^2)^{1/2}$, the modulus of the vector $(A_1, A_2, ..., A_M)$.

2.1.1. ModF on the P-map

If the noise is distributed normally and independently, the 1-pdf of d_j at any point of each image is

$$f(d_j(\vec{x})|A_j) = \frac{1}{\sqrt{2\pi}\sigma(\vec{x})} \exp\left[\frac{-(d_j(\vec{x}) - A_j\tau(\vec{x}))^2}{2\sigma^2(\vec{x})}\right] \tag{5}$$

where $\tau(\vec{x})$ is the known source profile at the corresponding point. Since the noise is independent between the different images, the M-pdf can be written as

$$f(d_1(\vec{x}), ..., d_M(\vec{x})|A_1, ..., A_M) = \frac{1}{(2\pi)^{M/2}\sigma^M(\vec{x})} \exp\left[-\sum_j \frac{(d_j(\vec{x}) - A_j\tau(\vec{x}))^2}{2\sigma^2(\vec{x})}\right]. \tag{6}$$

Next, we will derive the distribution of $P(\vec{x})$, the modulus of $(d_1(\vec{x}), d_2(\vec{x}), ..., d_M(\vec{x}))$. By changing to M-dimensional spherical coordinates, $(P, \theta_1, ..., \theta_{M-1})$, we write at any point $\vec{x}$, (in order to simplify the notation we write P instead of $P(\vec{x})$)

$$f(P, \theta_1, ..., \theta_{M-1}|A) = \frac{P^{M-1}}{(2\pi)^{M/2}\sigma^M} \exp\left[-\frac{P^2 + A^2\tau^2}{2\sigma^2} + \frac{PA\tau\cos\theta_{M-1}}{\sigma^2}\right] \times (\sin\theta_{M-1})^{M-2}(\sin\theta_{M-2})^{M-3} \ldots \sin\theta_2 \tag{7}$$

This is the joint pdf of the modulus P and the corresponding angles, note that $A \equiv (\sum_j A_j^2)^{1/2}$ and we have multiplied by the Jacobian of the coordinate change. Finally, by integrating on the angles $\theta_1, ..., \theta_{M-1}$, we find the pdf of the modulus P:

$$f(P|A) = \frac{P^{M/2}}{\sigma^2(A\tau)^{(M-2)/2}} \exp\left[-(A^2\tau^2 + P^2)/2\sigma^2\right] I_{\frac{M-2}{2}}\left(A\tau\frac{P}{\sigma^2}\right), \tag{8}$$

where $I_{(M-2)/2}$ is the modified Bessel function of the corresponding order. When M=2 we obtain the Rice distribution [20]. In the case $\sigma = 1$ with a general M, distribution (8) is the non-central chi distribution with M degrees of freedom and $\lambda = A\tau$ [21, 22]. This was expected since we have derived the pdf of the modulus of a vector whose components follow independent Gaussian distributions with mean $A_j\tau$. If there is no source, the previous formula defaults to

$$f(P|0) = \frac{MP^{M-1}}{2^{M/2}\sigma^M\Gamma(1 + M/2)} \exp\left[-P^2/2\sigma^2\right], \tag{9}$$

where Γ is the gamma function. In the case $\sigma = 1$, (9) is the chi distribution. In particular, when M=2 we obtain the Rayleigh distribution [23].

Now we assume that the M images are pixelized with the same pixel size; since the noise is independent pixel to pixel, the different values of P at each pixel, P_i, $i = 1, \ldots, N$, with N the number of pixels, follow the two distributions

$$f(P_1, .., P_N|0) = \prod_i \frac{M P_i^{M-1}}{2^{M/2}\sigma_i^M \Gamma(M/2+1)} \exp\left[-P_i^2/2\sigma_i^2\right] \qquad (H_o), \tag{10}$$

$$f(P_1, ..., P_N|A) = \prod_i \frac{P_i^{M/2} \exp\left[-\frac{A^2\tau_i^2+P_i^2}{2\sigma_i^2}\right]}{\sigma_i^2 (A\tau_i)^{\frac{M-2}{2}}} I_{\frac{M-2}{2}}\left(A\frac{P_i\tau_i}{\sigma_i^2}\right) \qquad (H_1), \tag{11}$$

being H_o and H_1 the null (absence of source) and the alternative (presence of source) hypotheses, respectively, and τ_i the profile at the i^{th} pixel. The log-likelihood is defined by

$$l(A|P_1, ..., P_N) = \log f(H_1) =$$
$$-A^2 \sum_i \frac{\tau_i^2}{2\sigma_i^2} - N(M-2)/2 \log A + \sum_i \log\left[I_{(M-2)/2}\left(A\frac{P_i\tau_i}{\sigma_i^2}\right)\right]. \tag{12}$$

Where we have only written the terms wich depend on A. The MLE of the amplitude, $\hat{A}$, can be obtained by maximizing the previous expression and is given by the solution of the equation

$$\hat{A} \sum_i \frac{\tau_i^2}{\sigma_i^2} = \sum_i y_i \frac{I_{M/2}(\hat{A}y_i)}{I_{(M/2-1)}(\hat{A}y_i)}, \quad y_i \equiv \frac{P_i\tau_i}{\sigma_i^2}. \tag{13}$$

This equation can be interpreted as a non-linear filter operating on the data (ModF). This method allows us to obtain the MLE of A given a total polarization map P.

2.1.2. Filtered Fusion (FF)

In this case we consider separately each one of the M images. We call d_{ji} the intensity in the j^{th} image at the i^{th} pixel and σ_i the dispersion at each pixel. The pdf of the intensities in the j^{th} image is

$$f(d_{j1}, ..., d_{jN}|A_j) = \frac{1}{(2\pi)^{N/2}\sigma_1.....\sigma_N} \exp\left[-\sum_i \frac{(d_{ji} - A_j\tau_i)^2}{2\sigma_i^2}\right]. \tag{14}$$

The MLE for A_j yields

$$\hat{A}_j = \frac{\sum_i d_{ji}\tau_i/\sigma_i^2}{\sum_i \tau_i^2/\sigma_i^2} \tag{15}$$

This is equivalent to the application of the linear matched filter MF, Φ, operating on each image d_j, as given by [24]:

$$\Phi(\vec{x}) \propto \frac{\tau(\vec{x})}{\sigma^2(\vec{x})}. \tag{16}$$

Then, with the M filtered images $\hat{A}_j$ we make the non-linear fusion $\hat{A} \equiv (\sum_j \hat{A}_j^2)^{1/2}$, in order to estimate the source polarization amplitude. We call this operation FF. Note that this method is clearly different from the ModF, now we calculate the MLE of each component A_j, given the values d_{ji} of that image and finally compute the modulus A of that estimated vector, whereas with the ModF we calculate the MLE of A given the polarization map P. For using the FF, we need to know all the images. On the other hand, for using the ModF we only need to know the total polarization map P.

2.1.3. Matched Fiter (MF)

This is a naive approach, assuming that we only know the P-map. We estimate A according to the expression

$$\hat{A} = \frac{\sum_i P_i \tau_i / \sigma_i^2}{\sum_i \tau_i^2 / \sigma_i^2} \tag{17}$$

with P_i the polarization data at each pixel. This simple technique can be useful for comparison with the more elaborated methods presented in the previous subsections.

2.2. The case of three images

Now, we shall assume that we have the same compact source in three images Q, U, V (this is the standard notation for Stokes parameters), characterized by amplitudes A_Q, A_U, A_V and a profile $\tau(\vec{x})$ immersed in noise $n_{Q,U,V}(\vec{x})$ that is Gaussian and independently distributed with zero mean and dispersion $\sigma(\vec{x})$. In general, we will consider that the noise is non-stationary. We will assume a linear model for the three images

$$Q, U, V(\vec{x}) = A_{Q,U,V}\tau(\vec{x}) + n_{Q,U,V}(\vec{x}). \tag{18}$$

The P-map, $P(\vec{x}) \equiv (Q^2(\vec{x}) + U^2(\vec{x}) + V^2(\vec{x}))^{1/2}$, is characterised by a source with amplitude $A \equiv (A_Q^2 + A_U^2 + A_V^2)^{1/2}$.

2.2.1. ModF on the P-map

In the case of three images, formulas (12) and (13) can be written as

$$l(A|P_1,...,P_N) = \log f(H_1) = -A^2 \sum_i \frac{\tau_i^2}{2\sigma_i^2} - N \log A + \sum_i \log\left[\sinh\left(A\frac{P_i\tau_i}{\sigma_i^2}\right)\right]. \quad (19)$$

$$\hat{A}\sum_i \frac{\tau_i^2}{\sigma_i^2} + \frac{N}{\hat{A}} = \sum_i y_i \coth(\hat{A}y_i), \quad y_i \equiv \frac{P_i\tau_i}{\sigma_i^2}. \quad (20)$$

This equation can be interpreted as a non-linear filter operating on the data which is the (ModF) for this particular case.

2.2.2. Filtered fusion (FF)

In this case, we use the same MF operating on each image Q, U, V, as given by equation (15). Then, with the three filtered images Q_{MF}, U_{MF}, V_{MF} we make the non-linear fusion $\hat{A} \equiv (Q_{MF}^2 + U_{MF}^2 + V_{MF}^2)^{1/2}$ pixel by pixel.

2.2.3. Matched Filter (MF)

We just apply (17) to the case of three images.

3. Simulations and results

As commented in the introduction, since the estimation of the intensity of polarized sources is of great interest in Astrophysics, we will use an example taken from CMB Astronomy in order to illustrate the performance of the techniques introduced in the previous section.

In order to compare and evaluate the performance of the two filters, we have simulated images of 16×16 pixels with a pixel angular size[1] of 3 arcmin. We simulate the Q, U and V components of the polarization as follows: each component consists of Gaussian uncorrelated noise, plus a polarized point source filtered with a Gaussian-shaped beam whose full width half maximum (FWHM) is 14 arcmin. This is a typical example of a CMB polarization experiment[2]. So the source polarization components can be written as

$$s_{Q,U,V} \equiv A_{Q,U,V} \exp\left[-\frac{|\vec{x}|^2}{2\gamma^2}\right], \quad (21)$$

[1]The angle of the sky subtended by a pixel of the detector, for a given telescope.

[2]This particular choice of the pixel and beam sizes corresponds to the specifications of the 70 GHz channel of the ESA's *Planck* satellite.

where γ is the beam dispersion (angular size) and we assume in this formula that the source is centered at the origin. We consider stationary noise,with zero mean and r.m.s. deviation $\sigma = 1$ in some unit system[3]. We take values of A_Q, A_U and A_V ranging from 0 to 2.5 with a step of 0.5. The number of simulations is 100 for each combination of triplets of values of A_Q, A_U and A_V. After carrying out the corresponding simulations for Q, U and V, we add them quadratically and take the square root to calculate $P = \sqrt{Q^2 + U^2 + V^2}$, the total polarization.

We assume that we do not know the exact position of the source in the map and then we place it at random in the image. We have considered images of 16×16 pixels in order to do fast calculations. In order to avoid border effects, we simulate and filter 24×24 pixel patches and, after the filtering step, we retain only the 16×16 pixel central square.

We use three different filters: the FF, as described in section 2.2.2), which consists in the application of the matched filter to the images in Q, U and V separately and then the calculation/construction of the P-map from the matched-filtered images, the ModF applied directly on P, derived from the MLE applied to the modulus distribution and presented with detail in section 2.2.1 and a simple MF applied on the P-map. We apply these filters to each simulation, centering the filters successively at each pixel, since we do not know the source position. We estimate the source amplitude A_{ModF} for the ModF, in this case we calculate the value of A which maximises the log-likelihood, eq. (19). For the FF we estimate separately and obtain $A_{FF} = \sqrt{Q_{MF}^2 + U_{MF}^2 + V_{MF}^2}$. With the MF, we obtain the estimator of A, (17). Then, we have constructed three maps (one for the ModF , one for the FF and another one for the MF) with the estimated values of A at each pixel.

We show in Figure 1 four images corresponding to a polarized source with $(A_Q, A_U, A_V) = (1.5, 1.5, 1.5)$ embedded in noise. For the sake of a better visualisation, we show 48×48 pixel images instead of the 16×16 sized images used in the simulations. We show the original image in P including noise and source, the image of the source, the image filtered with the ModF and finally, the image treated with the FF method. As we will comment with more detail below, the performance of the MF is much worse than that of the other filters and we will only show some results obtained with the MF, leaving the figures and tables for the comparison of the FF and the ModF.

We compute the absolute maximum of each filtered map (A_{ModF}, A_{FF} and A_MF) and keep this value as the estimated value of the polarization amplitude of the source and the position of the maximum as the position of the source. Note that for the more realistic case where more than one source can be present in the images, it is still possible to proceed as

[3]For this example, we use arbitrary intensity units, since the quantity of interest for our purposes is the signal to noise ratio of the sources.

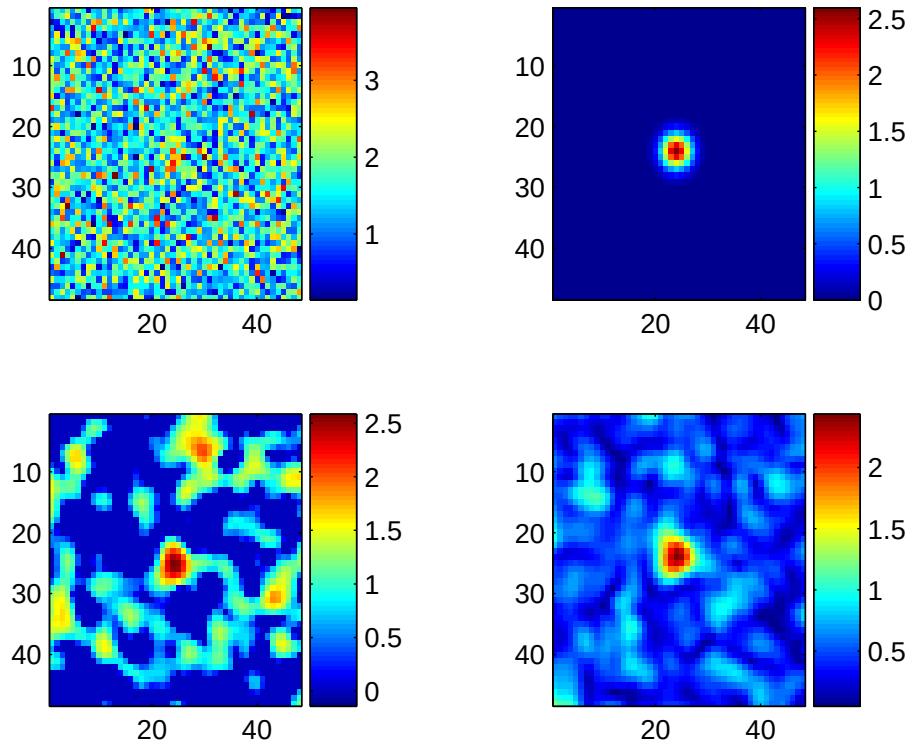

Figure 1: Top left: Image of a polarized source filtered with a Gaussian beam. The source polarization components are $(A_Q, A_U, A_V) = (1.5, 1.5, 1.5)$ and it is embedded in stationary noise $\sigma = 1$. Top right: Image of the polarized source only. Bottom left: The first image after application of the ModF. Bottom right: The first image after the application of the FF.

described by looking for local peaks in the filtered images.

We also calculate the significance level of each detection. In order to do this, we carry out 1000 simulations with $A_Q = 0$, $A_U = 0$, $A_V = 0$ and we calculate the estimated value of the source polarization in this case for each filter. We consider the null hypothesis H_0 (there is no polarized source) against the alternative hypothesis H_1 (there is a polarized source). We set a significance level $\alpha = 0.05$; this means that we reject the null hypothesis when a simulation has a estimated source polarization amplitude higher than that of 95% of the simulations without polarized source. The previous significance fixes a lower threshold ($A_* = 1.99$ for the ModF and $A_* = 1.17$ for the FF and $A_* = 3.81$ for the MF) defining a region of acceptance in the space of polarization amplitudes. We define the power of the

test as $1-\delta$, with δ the probability of accepting the null hypothesis when it is false, i.e. the power is the proportion of simulations with polarized source with a estimated amplitude higher than that of A_*. The higher the power the more efficient the filter is for detection.

We calculate the estimated value of the polarization amplitude $\hat{A}$ and compare it with the real value A, obtaining the relative error of the estimation and its absolute value for each simulation.We also calculate the estimated position of the detected source and obtain the position error expressed in terms of the number of pixels. The average of all these quantities for 100 simulations are presented in Table 1 for all the cases. The rows in the Table are sorted in ascending order of A. We see in the table that the power for the FF is higher than for the ModF. The improvement is particularly high for A values equal or lower than 2.5. In this case the position and polarization errors are also lower for the FF. The FF can detect sources from $A \geq 1.8$ with power ≥ 0.99 and average relative error (bias) ≤ 0.05, average of its absolute value ≤ 0.14 and average position error ≤ 0.53. For $A = 1.8$, the ModF detects with power = 0.41, average relative error = 0.25, average of its absolute value = 0.25 and average position error = 1.39. For $A = 1.8$, the MF detects with power = 0.46, average relative error = 1.20, average of its absolute value = 1.20 and average position error = 1.34. The errors of the polarization estimation for the MF are much higher than for the other methods, whereas the power and the position error are similar to those obtained with the ModF.

The ModF and the FF perform in a similar way for signal-to noise ratio $A \geq 3$, in this case the power is 1 for both filters and the bias is ≤ 0.02. The ModF is also slower than the FF, due to the maximization process involved in its application. However, note that the FF cannot be applied when we only have the image of the modulus i.e. we do not have information about the components, in this case the ModF can be a suitable filter, specially for signal-to-noise ratio ≥ 3.

In Figure 2, we have plotted the estimated polarization amplitude $\hat{A}$ against the real polarization amplitude A for the ModF and the FF. The average and 68% confidence intervals of 100 simulations are shown. It is clear that the FF performs better till $A \cong 3$. In Figure 1, we can also see the better performance of the FF. From a qualitative point of view, the ModF image shows more structure, with bright artifacts that could lead to spurious detections, while the FF image looks smoother. This is easy to understand if we think ModF is enhancing an inherently non-Gaussian noise, whereas FF is the (non linear) composition of three smoothed Gaussian noises.

Finally, we have plotted in Figure 3 the position error in numbers of pixels for 1000 simulations in the particular case $A_Q = 0.5$, $A_U = 1$, $A_V = 1$. Only the simulations with a significance $\alpha = 0.05$ have been taken into account and represented. It is clear that the position error is lower for the FF.

In order to try to understand the better performance of the FF, we have carried out

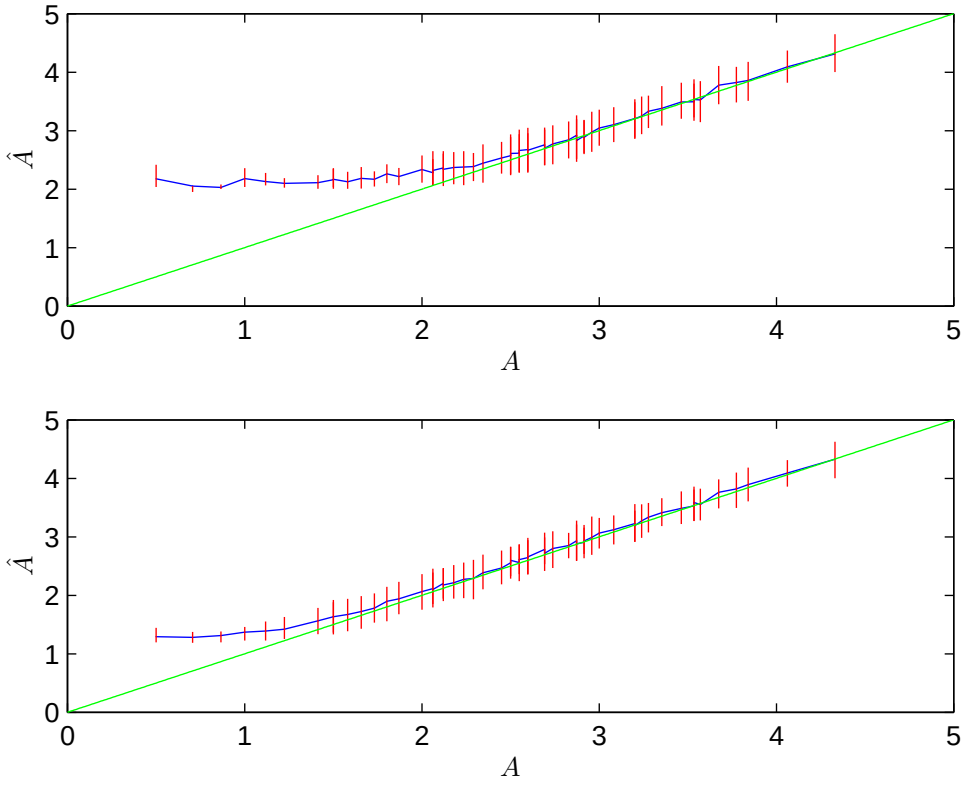

Figure 2: Estimated source polarization amplitude $\hat{A}$ plotted against the real polarization amplitude A. The average and 68% confidence intervals of 100 simulations are plotted. Top : the ModF has been used. Bottom: the FF has been applied. The straight line $\hat{A} = A$ has been drawn for comparison.

simulations of three-dimensional vectors whose components are gaussian-distributed with dispersion $\sigma = 1$ and values of the mean ranging from 0.5 to 2.5. We have considered the ModF, i.e we find the value of A which maximizes (8) with $\tau = 1$ and the filtered fusion, which amounts to averaging the components and calculating the modulus of this average vector; this last method is also considered in [11] for the 2-dimensional case. The conclusion for these simple cases is that the FF performs better than the ModF, specially for the low signal-to-noise case, i.e. these simple examples confirm our conclusions: it is more precise to estimate the modulus estimating first the components and then calculating the square root of the quadratic sum than calculating the MLE estimator directly on the modulus.

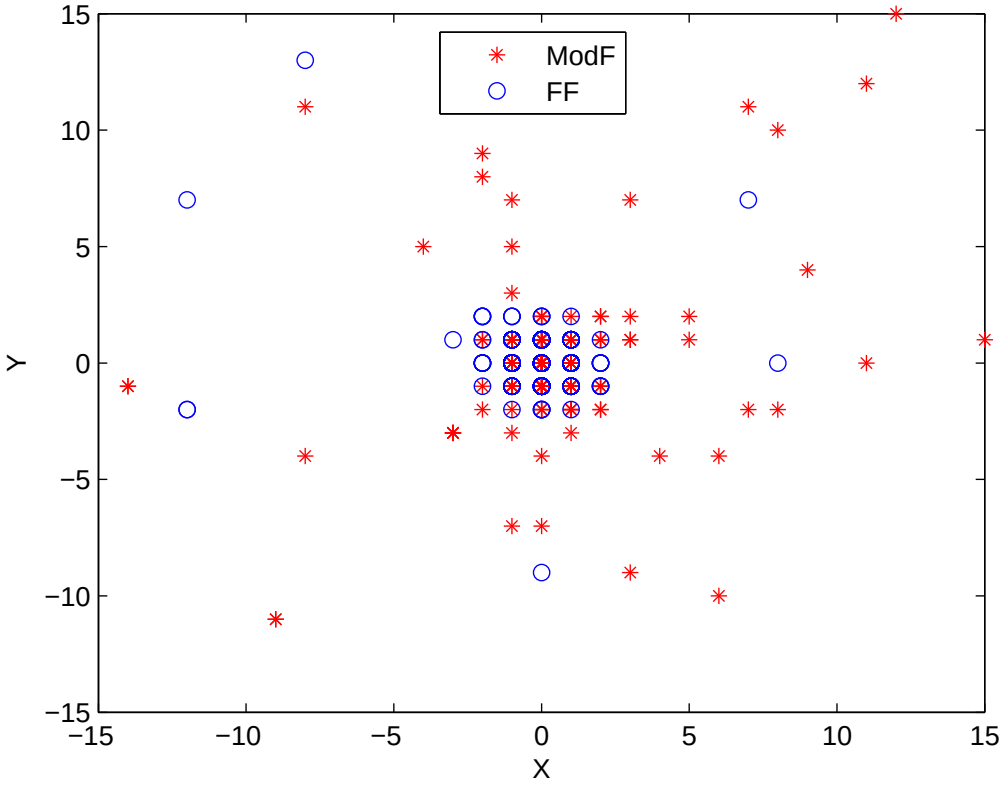

Figure 3: Position error in number of pixels for the case $A_Q = 0.5$, $A_U = 1$, $A_V = 1$. 1000 simulations have been considered.

4. Conclusions

In this paper, we deal with the detection and estimation of the modulus of a vector, a problem of great interest in general and in particular in astrophysics when we consider the polarization of the cosmic microwave background (CMB), extragalactic sources, the interestellar medium or the Sun. The total polarization intensity P is defined as $P \equiv (Q^2 + U^2 + V^2)^{1/2}$, where Q , U (linear polarization) and V (circular polarization) are the Stokes parameters. We consider the case of images in Q, U and V consisting of a compact source with a profile $\tau(\vec{x})$ immersed in Gaussian uncorrelated noise. We intend to detect the source and estimate its polarization amplitude by using three different methods, two new and a standard matched filter. a) a filter operating on the modulus P (ModF) and based on the maximization of the corresponding log-likelihood and b) a filtered fusion (FF) procedure, i.e. the application of the matched filter (MF) on the images of Q, U and

V and the combination of the corresponding estimates by making the non-linear fusion $\hat{A} \equiv (Q^2_{MF} + U^2_{MF} + V^2_{MF})^{1/2}$ and c) a matched filter (MF) operating on the P-map. We present the three filters in Section 2 for the general case of the modulus of a M-vector, and for the case of three-dimensional vectors, deriving the corresponding expressions , eqs. (13) and (20), for the estimation of the modulus of a vector with the ModF.

Since we are interested in the detection of polarized signals in Astrophysics, we have only considered the three-dimensional vector case in our simulations. Note, however that the methods can be applied in the general case of combination of M images to obtain the image of the modulus of a vector.

We have compared the performance of the filters when applied to simulated images consisting of the Q, U and V components of a Gaussian-shaped signal with different intensities plus Gaussian uncorrelated stationary noise. For each simulation and for the two methods, we have estimated the source amplitude and position. Besides, we have calculated the detection power for a fixed significance $\alpha = 0.05$ and the errors of the estimated amplitude and position. We find that the performance of the FF is the best for low signal-to-noise, the ModF performs like the FF for $A \geq 3$. The MF produces very high errors in the polarization estimation, making this filter unsuitable for the treated problem.

We want to point out the good performance of the ModF, which could be an interesting alternative to the FF when we have an image of the modulus, but we do not know the components of the vector.

Finally, it would be interesting to generalize our methods to the case of images in which the noise at different pixels is not uniform or, more generally, is correlated. This could be important for CMB polarization observations. We leave this problem for further work.

Acknowledgments

The authors acknowledge partial financial support from the Spanish Ministry of Education (MEC) under project ESP2004-07067-C03-01 and from the joint CNR-CSIC research projects 2006-IT-0037 and 2008-IT-0059.

[1] W. Nailong, Using a matched filter to improve SNR of radio maps., in: D. M. Worrall, C. Biemesderfer, J. Barnes (Eds.), Astronomical Data Analysis Software and Systems I, Vol. 25 of Astronomical Society of the Pacific Conference Series, 1992, pp. 291–293.

[2] D. Herranz, J. L. Sanz, M. P. Hobson, R. B. Barreiro, J. M. Diego, E. Martínez-González, A. N. Lasenby, Filtering techniques for the detection of Sunyaev-Zel'dovich clusters in multifrequency maps, Monthly Notices of the Royal As-

Table 1: First column: triplets of values of A_Q, A_U and A_V and the corresponding value of A in σ units. Second and third columns: detection power for the ModF and FF (percentage) for a significance level α = 0.05. Fourth and fifth columns: flux relative errors for the two filters. Sixth and seventh columns: absolute value of the relative error. Eighth and ninth columns: position errors in numbers of pixels. In all the cases we have performed the average of 100 simulations.

$(A_Q, A_U, A_V; A)$	$\mathbf{pow}_{ModF}$	$\mathbf{pow}_{FF}$	$\mathbf{err}_{ModF}$	$\mathbf{err}_{FF}$	$\mathbf{\lvert err\rvert}_{ModF}$	$\mathbf{\lvert err\rvert}_{FF}$	$\mathbf{pos}_{ModF}$	$\mathbf{pos}_{FF}$
(0.00,0.00,0.50;0.50)	6	12	3.35	1.58	3.35	1.58	4.36	3.83
(0.00,0.50,0.50;0.71)	1	22	1.90	0.81	1.90	0.81	11.31	2.45
(0.50,0.50,0.50;0.87)	7	41	1.34	0.52	1.34	0.52	6.68	2.19
(0.00,0.00,1.00;1.00)	5	47	1.18	0.37	1.18	0.37	3.80	1.99
(0.00,0.50,1.00;1.12)	6	71	0.91	0.24	0.91	0.24	3.44	1.23
(0.50,0.50,1.00;1.22)	6	76	0.71	0.16	0.71	0.17	3.11	1.14
(0.00,1.00,1.00;1.41)	17	89	0.49	0.10	0.49	0.14	3.24	0.87
(0.00,0.00,1.50;1.50)	24	96	0.45	0.09	0.45	0.15	2.34	0.70
(0.50,1.00,1.00;1.50)	25	95	0.44	0.09	0.44	0.15	2.17	0.65
(0.00,0.50,1.50;1.58)	27	96	0.34	0.06	0.34	0.14	1.45	0.62
(0.50,0.50,1.50;1.66)	27	97	0.32	0.04	0.32	0.13	1.37	0.61
(1.00,1.00,1.00;1.73)	43	100	0.25	0.03	0.25	0.11	1.53	0.70
(0.00,1.00,1.50;1.80)	41	99	0.25	0.05	0.25	0.14	1.39	0.43
(0.50,1.00,1.50;1.87)	50	100	0.18	0.04	0.18	0.12	1.33	0.53
(0.00,0.00,2.00;2.00)	59	100	0.17	0.03	0.17	0.12	0.83	0.30
(0.00,0.50,2.00;2.06)	63	100	0.12	0.02	0.13	0.12	0.72	0.40
(1.00,1.00,1.50;2.06)	65	100	0.11	0.03	0.11	0.10	0.92	0.41
(0.00,1.50,1.50;2.12)	76	100	0.11	0.04	0.12	0.10	0.61	0.33
(0.50,0.50,2.00;2.12)	74	100	0.10	0.03	0.12	0.10	0.66	0.35
(0.50,1.50,1.50;2.18)	76	100	0.09	0.02	0.11	0.11	0.73	0.33
(0.00,1.00,2.00;2.24)	81	100	0.06	0.02	0.10	0.10	0.62	0.33
(0.50,1.00,2.00;2.29)	81	100	0.04	0.00	0.09	0.10	0.79	0.31
(1.00,1.50,1.50;2.35)	86	100	0.04	0.02	0.11	0.10	0.90	0.22
(1.00,1.00,2.00;2.45)	85	100	0.03	0.01	0.09	0.09	0.56	0.24
(0.00,0.00,2.50;2.50)	96	100	0.04	0.04	0.10	0.09	0.51	0.18
(0.00,1.50,2.00;2.50)	96	100	0.03	0.02	0.10	0.09	0.50	0.25
(0.00,0.50,2.50;2.55)	95	100	0.04	0.02	0.11	0.09	0.48	0.24
(0.50,1.50,2.00;2.55)	94	100	0.03	0.00	0.10	0.10	0.68	0.20
(0.50,0.50,2.50;2.60)	99	100	0.03	0.02	0.10	0.09	0.58	0.17
(1.50,1.50,1.50;2.60)	95	100	0.03	0.02	0.11	0.10	0.62	0.17
(1.00,1.50,2.00;2.69)	99	100	0.02	0.03	0.10	0.08	0.49	0.16
(0.00,1.00,2.50;2.69)	97	100	0.00	0.01	0.09	0.08	0.50	0.14
(0.50,1.00,2.50;2.74)	98	100	0.01	0.02	0.10	0.09	0.38	0.15
(0.00,2.00,2.00;2.83)	100	100	0.00	0.01	0.09	0.06	0.58	0.15
(1.00,1.00,2.50;2.87)	99	100	-0.01	0.00	0.10	0.08	0.44	0.17
(0.50,2.00,2.00;2.87)	98	100	0.02	0.02	0.11	0.09	0.41	0.15
(0.00,1.50,2.50;2.92)	100	100	-0.01	0.01	0.08	0.06	0.32	0.09
(1.50,1.50,2.00;2.92)	100	100	0.00	0.00	0.08	0.08	0.35	0.10
(0.50,1.50,2.50;2.96)	100	100	0.01	0.01	0.09	0.08	0.33	0.11
(1.00,2.00,2.00;3.00)	100	100	0.01	0.02	0.08	0.07	0.27	0.07
(1.00,1.50,2.50;3.08)	100	100	0.01	0.01	0.08	0.06	0.27	0.05
(0.00,2.00,2.50;3.20)	100	100	0.00	0.00	0.08	0.07	0.33	0.12

tronomical Society 336 (2002) 1057–1068. arXiv:arXiv:astro-ph/0203486, doi:10.1046/j.1365-8711.2002.05704.x.

[3] D. Herranz, J. L. Sanz, Matrix Filters for the Detection of Extragalactic Point Sources in Cosmic Microwave Background Images, IEEE Journal of Selected Topics in Signal Processing 5 (2008) 727–734. arXiv:0808.0300, doi:10.1109/JSTSP.2008.2005339.

[4] J. L. Sanz, D. Herranz, M. López-Caniego, F. Argüeso, Wavelets on the sphere. Application to the detection problem, in: Proceedings of the 14th European Signal Processing Conference (2006)., EUSIPCO 2006 Conference, 2006, pp. 1–5.

[5] J. González-Nuevo, F. Argüeso, M. López-Caniego, L. Toffolatti, J. L. Sanz, P. Vielva, D. Herranz, The Mexican hat wavelet family: application to point-source detection in cosmic microwave background maps, Monthly Notices of the Royal Astronomical Society 369 (2006) 1603–1610. arXiv:arXiv:astro-ph/0604376, doi:10.1111/j.1365-2966.2006.10442.x.

[6] M. López-Caniego, D. Herranz, R. B. Barreiro, J. L. Sanz, Filter design for the detection of compact sources based on the Neyman-Pearson detector, Monthly Notices of the Royal Astronomical Society 359 (2005) 993–1006. arXiv:arXiv:astro-ph/0503148, doi:10.1111/j.1365-2966.2005.08961.x.

[7] M. López-Caniego, J. González-Nuevo, D. Herranz, M. Massardi, J. L. Sanz, G. De Zotti, L. Toffolatti, F. Argüeso, Nonblind Catalog of Extragalactic Point Sources from the Wilkinson Microwave Anisotropy Probe (WMAP) First 3 Year Survey Data, The Astrophysical Journal Supplement Series 170 (2007) 108–125. arXiv:arXiv:astro-ph/0701473, doi:10.1086/512678.

[8] S. M. Leach, J. Cardoso, C. Baccigalupi, R. B. Barreiro, M. Betoule, J. Bobin, A. Bonaldi, J. Delabrouille, G. de Zotti, C. Dickinson, H. K. Eriksen, J. González-Nuevo, F. K. Hansen, D. Herranz, M. Le Jeune, M. López-Caniego, E. Martínez-González, M. Massardi, J. Melin, M. Miville-Deschênes, G. Patanchon, S. Prunet, S. Ricciardi, E. Salerno, J. L. Sanz, J. Starck, F. Stivoli, V. Stolyarov, R. Stompor, P. Vielva, Component separation methods for the PLANCK mission, Astronomy & Astrophysics 491 (2008) 597–615. arXiv:0805.0269, doi:10.1051/0004-6361:200810116.

[9] J. A. Tauber, The Planck Mission, in: A. N. Lasenby, A. Wilkinson (Eds.), New Cosmological Data and the Values of the Fundamental Parameters, Vol. 201 of IAU Symposium, 2005, pp. 86–+.

[10] P. Carvalho, G. Rocha, M. P. Hobson, A fast Bayesian approach to discrete object detection in astronomical data sets - PowellSnakes I, Monthly Notices of the Royal Astronomical Society 393 (2009) 681–702. arXiv:0802.3916, doi:10.1111/j.1365-2966.2008.14016.x.

[11] L. Oberto, F. Pennecchi, Estimation of the modulus of a complex-valued quantity, Metrologia 43 (6) (2006) 531.
URL http://stacks.iop.org/0026-1394/43/i=6/a=008

[12] J. F. L. Simmons, B. G. Stewart, Point and interval estimation of the true unbiased degree of linear polarization in the presence of low signal-to-noise ratios, Astronomy & Astrophysics 142 (1985) 100–106.

[13] J. F. C. Wardle, P. P. Kronberg, The linear polarization of quasi-stellar radio sources at 3.71 and 11.1 centimeters, The Astrophysical Journal 194 (1974) 249–255. doi:10.1086/153240.

[14] A. Cooray, A. Melchiorri, J. Silk, Is the cosmic microwave background circularly polarized?, Physics Letters B 554 (2003) 1–2. arXiv:arXiv:astro-ph/0205214, doi:10.1016/S0370-2693(02)03291-4.

[15] M. Kamionkowski, A. Kosowsky, A. Stebbins, Statistics of cosmic microwave background polarization, Phys. Rev. D 55 (12) (1997) 7368–7388. doi:10.1103/PhysRevD.55.7368.

[16] F. Argüeso, J. L. Sanz, D. Herranz, M. López-Caniego, J. González-Nuevo, Detection/estimation of the modulus of a vector. Application to point-source detection in polarization data, Monthly Notices of the Royal Astronomical Society 395 (2009) 649–656. arXiv:0906.0893, doi:10.1111/j.1365-2966.2009.14549.x.

[17] J. G. Kirk, O. Tsang, High brightness temperatures and circular polarisation in extra-galactic radio sources, Astronomy & Astrophysics 447 (2006) L13–L16. arXiv:arXiv:astro-ph/0512573, doi:10.1051/0004-6361:200500231.

[18] A. Tritschler, D. A. N. Müller, R. Schlichenmaier, H. J. Hagenaar, Fine Structure of the Net Circular Polarization in a Sunspot Penumbra, The Astrophysical Journal Letters 671 (2007) L85–L88. arXiv:0710.4545, doi:10.1086/524872.

[19] N. L. J. Cox, N. Boudin, B. H. Foing, R. S. Schnerr, L. Kaper, C. Neiner, H. Henrichs, J.-F. Donati, P. Ehrenfreund, Linear and circular polarisation of diffuse interstellar bands, Astronomy & Astrophysics 465 (2007) 899–906. doi:10.1051/0004-6361:20065278.

[20] S. O. Rice, Selected Papers on Noise and Stochastic Processes, Dover Pubns, 1954, Ch. Mathematical analysis of random noise, pp. 133–294.

[21] P. L. Meyer, The maximum likelihood estimate of the non-centrality parameter of a non-central χ^2 variate, J. Am. Stat. Assoc. 62 (1967) 1258–1264.

[22] D. A. Anderson, Maximum likelihood estimation in the noncentral chi-distribution with unknown scale parameter, The Indian J. Stat. Series B 43 (1981) 58–67.

[23] A. Papoulis, Probability, Random Variables, and Stochastic Processes, Mc-Graw Hill, 1984.

[24] F. Argüeso, J. L. Sanz, Filter design for the detection of compact sources embedded in non-stationary noise plus a deterministic background, in: Proceedings of the 16th European Signal Processing Conference (2008), EUSIPCO 2008 Conference, Lausanne, Switzerland, 2008, pp. 1–5.